*European COST F3 Conference on System Identification & Structural Health Monitoring,* Universidad Politecnica de Madrid, Spain, 6-9 June 2000.

# MODAL EXPANSION MODELING OF THE ELECTRO-MECHANICAL (E/M) IMPEDANCE RESPONSE OF 1-D STRUCTURES

Victor Giurgiutiu and Craig A. Rogers

Department of Mechanical Engineering, University of South Carolina, Columbia, SC 29208
Phone: 803-777-8018, FAX: 803-777-0106, E-mail*: victorg@sc.edu*

**SUMMARY**: The electro-mechanical (E/M) impedance response of a 1-D structure interrogated by a PZT wafer active sensor is modeled from first principles. Equations of motion for the flexural vibrations under moment excitation from the PZT wafer are developed. Solution in terms of normal modes with internal damping is obtained. General expressions for pointwise dynamic stiffness and pointwise dynamic compliance are developed. Effective stiffness of the PZT wafer is also calculated, and the complex stiffness ratio for the PZT-structure interaction is determined. Hence, the complex electro-mechanical impedance and admittance are deduced. A numerical example is given to illustrate the method and test its effectiveness. At structural resonance frequencies, the interaction between the real part of the structural dynamic stiffness and the PZT stiffness is directly reflected in the real part of the electro-mechanical impedance. The same behavior is also found in the electro-mechanical admittance. Both reflect the change in structural response, due to the presence of damage and internal flaws.

**KEYWORDS**: Structural health monitoring; piezoelectric; active sensors; ultrasonics; damage detection; modal analysis; smart structures, electro-mechanical impedance.

## INTRODUCTION

Health monitoring of structures and machinery is a major concern of the engineering community. Flaws identification, early damage detection, and failure prevention are desiderates with far reaching implications in the management and preservation of nations aging infrastructure. Among structural health monitoring techniques, the electro-mechanical (E/M) impedance for structural health monitoring and non-destructive evaluation is an emerging method that offers distinct advantages. The electro-mechanical (E/M) impedance method has gained acceptance as an effective technique for structural health monitoring, damage detection, and failure prevention (Giurgiutiu and Rogers, 1998). The method uses small-size active sensors intimately bonded to an existing structure, or embedded into a new composite construction. Piezoelectric (PZT) wafer transducers have been widely used to this purpose. Experimental demonstrations have shown that the real part of the high-frequency impedance spectrum is directly affected by the presence of damage or defects in the monitored structure (Figure 1).

A precursor to the electromechanical impedance method is the mechanical impedance method. Currently, ultrasonic equipment manufacturers offer mechanical impedance analysis (MIA) probes and equipment as standard options (e.g., Staveley NDT Technologies, 1998). The mechanical impedance method is used to detect disbonds in laminated structures, and delaminations inside composite materials up to depth of 1/4-in. The electro-mechanical

impedance method takes the mechanical impedance concepts to the new horizons offered by the use of small-wafer piezoelectric active sensors intimately affixed to the structure. Force excitation normal to the structural surface is replaced by strain excitation in the plane of the surface. High frequency excitation in the high kHz low MHz region can be achieved. The bulky ultrasonic transducer of the mechanical impedance method (typically, 1" x 3-4") is replaced by a thin wafer active sensor. In addition, since the E/M impedance sensor is permanently attached to the surface (or embedded in composite structures), the force coupling issue associated with conventional ultrasonics is no longer a problem. The E/M impedance active sensors, hard wired into the structure, can be interconnected into sensor arrays. Through the intimate electro-mechanical coupling, the structural impedance is measured almost directly, whereas in the mechanical impedance method, post-processing of separately measured force and acceleration or velocity data was required.

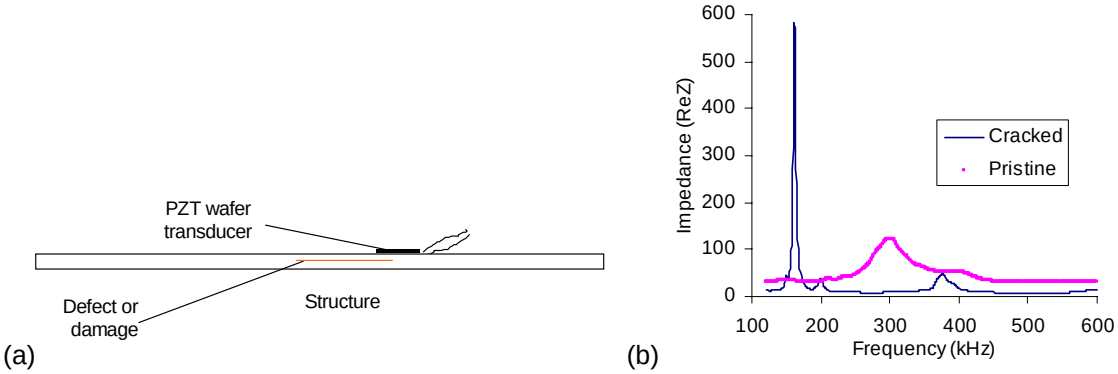


Figure 1 PZT wafer transducer acting as active sensor to monitor structural damage: (a) mounting of the PZT wafer transducer on a damaged structure; (b) the change in E/M impedance due to the presence of a crack.

Until now, the electro-mechanical impedance technique has evolved mainly through experimental discovery and proof-of-concept demonstrations. However, little theoretical work has been done so far to determine the analytical model that will permit to correctly predict the E/M impedance response for a given structure and its change with the progression of damage. Rossi *et al.* (1993) studied impedance modeling of piezoelectric actuator driven circular rings, but their analysis did not determine closed form solution. Their numerical examples were confined to relatively low frequencies (< 1.8 kHz). Liang *et al.* (1996) developed the impedance analysis of a PZT affixed to a structure, but did not detail a model for the structural response. Esteban (1996) attempted an analysis of beam vibrations with attached PZT wafers, but could not get fully conclusive results. The present paper focuses on modeling the interaction between the PZT wafer transducer and the structure in terms of high-frequency vibration modes through the point-wise structural impedance which is directly affected but the presence of local damage.

## ELECTRO-MECHANICAL IMPEDANCE

Consider a piezo-electric transducer wafer intimately bonded to the structural surface (Figure 1a). When excited by an alternating electric voltage, the piezo-electric transducer applies a local strain parallel to the surface. Thus, elastic waves are transmitted into the structure. The structure responds to the transducer excitation by presenting the drive-point dynamic stiffness $k_{str}(\omega) = -\omega^2 m_e(\omega) + i\omega c_e(\omega) + k_e(\omega)$. Through the mechanical coupling between the PZT

transducer and the host structure, and through the electro-mechanical transduction inside the PZT transducer, the structural drive-point dynamic stiffness gets reflected into the effective electrical impedance as seen at the transducer terminals (Figure 2). The electro-mechanical (E/M) impedance technique for health monitoring, damage detection, and NDE (Rogers and Giurgiutiu, 1997) utilizes the changes that take place in the drive-point structural impedance to identify incipient damage in the structure. The apparent E/M admittance, $Y(\omega)$, and E/M impedance, $Z(\omega)$, of the piezo-transducer coupled to the host structure are given by

$$Y(\omega) = i\omega C\left(1-\kappa_{31}^2 \frac{k_{str}(\omega)}{k_{PZT}+k_{str}(\omega)}\right), \qquad Z(\omega) = \frac{1}{i\omega C}\left(1-\kappa_{31}^2 \frac{k_{str}(\omega)}{k_{PZT}+k_{str}(\omega)}\right)^{-1} \tag{1}$$

where $C$ is the zero-load capacitance of the PZT transducer, $\kappa_{31}$ is the electro-mechanical cross coupling coefficient of the PZT transducer ( $\kappa_{31} = d_{13}/\sqrt{\bar{s}_{11}\bar{\varepsilon}_{33}}$ ), $k_{str}(\omega)$ is the dynamic stiffness of the structure, and $k_{PZT}$ is the dynamic stiffness of the PZT-wafer active sensor. The E/M impedance method is applied by scanning a predetermined frequency range in the hundreds of kHz band and recording the complex impedance spectrum. By comparing the impedance spectra taken at various times during the service life of a structure, meaningful information can be extracted pertinent to structural degradation and the appearance of incipient damage (Figure 1b). The frequency range must be high enough for the signal wavelength to be significantly smaller than the defect size.

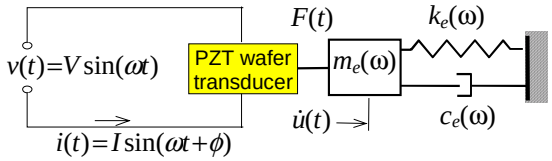


Figure 2 Electro-mechanical coupling between PZT transducer and structure.

The purpose of the present investigation is to determine an analytical model for predicting the structure and PZT contributions to Equation (1). Such model will permit prediction of the E/M impedance, $Z(\omega)$, for a given structure, will allow determination of the method sensitivity to detect a certain defect size, and will permit the matching of sensor size and excitation level with structural type and defect size. This paper gives a brief presentation of the subject and outlines the main findings. Full details of this work can be found in a report by Giurgiutiu and Rogers (1999).

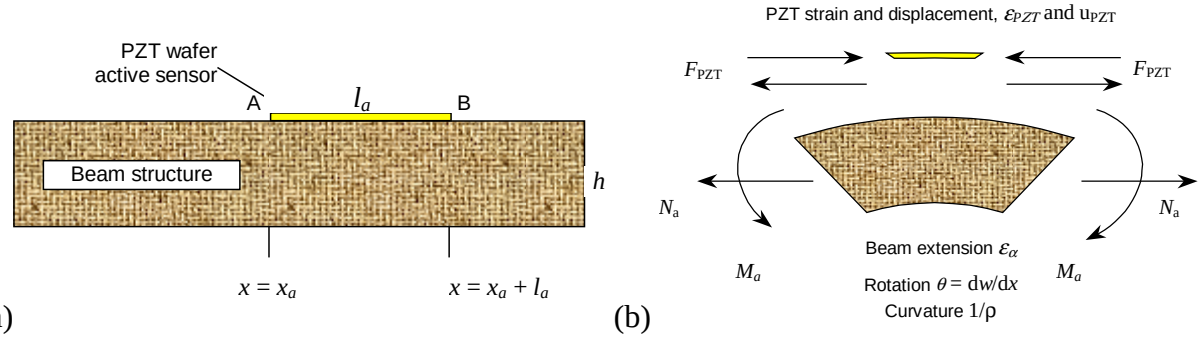


Figure 3 Interaction between PZT active sensor and a substructure: (a) geometry; (b) forces and moments.

## MODEL DEFINITION

Consider a beam structure with a PZT active sensor attached to it surface (Figure 3a). The PZT active sensor has length $l_a$, and lies between $x_a$ and $x_a + l_a$. Upon activation, the PZT active sensor expands by $\varepsilon_{PZT}$. This generates a reaction force $F_{PZT}$ from the beam onto the PZT and an equal and opposite force from the PZT onto the beam (Figure 3b). This force excites the beam. At the neutral axis, the effect is felts as an axial force excitation, $N_{PZT}$, and a bending moment excitation, $M_{PZT}$. As the active sensor is electrically excited with a high-frequency harmonic signal, it will induce elastic waves into the beam structure. The elastic waves travel sideways into the beam structure, and set it up into oscillation. In a steady-state regime, the structure oscillates at the PZT excitation frequency. The reaction force per unit displacement (dynamic stiffness) presented by the structure to the PZT will depend on the internal state of the structure, on the excitation frequency, and on the boundary conditions:

$$k_{str}(\omega) = \hat{F}_{PZT}(\omega) / \hat{u}_{PZT}(\omega), \tag{2}$$

where $\hat{u}_{PZT}(\omega)$ is the displacement amplitude at frequency ω, $\hat{F}_{PZT}(\omega)$ is the reaction force, and $k_{str}(\omega)$ is the dynamic stiffness. The symbol ^ signifies amplitude. Since the size of the PZT is very small with respect to the size of the structure, formula (2) represents a point-wise structural stiffness.

## MODELING OF THE STRUCTURAL SUBSTRATE

The response of the structural substrate to the PZT excitation is deduced following the general theory of beam vibrations (Timoshenko, 1955; Inman, 1996.) However, the PZT excitation departs from the typical textbook formulation since it acts a pair of self-equilibrating axial forces and bending moments that are separated by a small finite distance, $l_{PZT}$. This feature give *gusto* to our analysis.

### Definition of the Excitation Forces and Moments

The excitation forces and moments acting upon the beam structure are derived from the PZT force, $F_{PZT} = \hat{F}_{PZT} e^{i\omega t}$, using the beam cross-section geometry (Figure 3b):

$$M_a = F_{PZT} \frac{h}{2}, \quad N_a = F_{PZT} \tag{3}$$

The space-wise distribution of excitation bending moment and axial force are expressed using the Heaviside function, $H(x - x_a)$, defined as $H(x - x_a) = 0$ for $x < x_a$, and $H(x - x_a) = 1$ for $x_a \le x$:

$$N_e(x,t) = N_a \left[ H(x - x_a) - H(x - x_a - l_a) \right] \cdot e^{i\omega t} \tag{4}$$

$$M_e(x,t) = M_a \left[ H(x - x_a) - H(x - x_a - l_a) \right] \cdot e^{i\omega t} \tag{5}$$

Equations (5) and (6) correspond to axial and flexural vibrations, respectively. Axial vibrations modes are usually of much larger frequency than flexural vibration modes. They will not be considered in the present analysis.

**Flexural Vibrations**

For Euler-Bernoulli beams, the equation of motion under moment excitation is:

$$\rho A \cdot \ddot{w}(x,t) + EI \cdot w^{////}(x,t) = -M_e^{//}(x,t) \tag{6}$$

Substitution of Equation (6) into (7) yields:

$$\rho A \cdot \ddot{w}(x,t) + EI \cdot w^{////}(x,t) = -\hat{M}_a \left[ \delta^{/}\left(x - x_a\right) - \delta^{/}\left(x - x_a - l_a\right) \right] \cdot e^{i\omega t} \tag{7}$$

where $\delta'$ is the first derivative of Dirac's function ($\delta' = H''$). Assume modal expansion solution $w(x,t) = \sum_{n=N_1}^{N_2} C_n X_n(x) \cdot e^{i\omega t}$, with $C_n$ the modal amplitudes, $X_n(x)$ the mode shapes, and $N_1$, $N_2$ the lower and upper mode numbers bracketing the high-frequency interval under investigation. Since the mode shapes satisfy the free-vibration differential equation $EI \cdot X_n^{////} = \omega_n^2 \cdot \rho A \cdot X_n$, multiplication by $X_n(x)$ and integration over the length of the beam yields:

$$C_n = -\frac{1}{\omega_n^2 - \omega^2} \cdot \frac{\hat{M}_a}{\rho A} \int_0^l X_n(x) \left[ \delta^{/}\left(x - x_a\right) - \delta^{/}\left(x - x_a - l_a\right) \right] \mathrm{d}x \tag{8}$$

Upon integration by parts and substitution of Equation (4),

$$C_n = \frac{\hat{F}_{PZT}}{\rho A} \cdot \frac{h}{2} \cdot \frac{X_n^{/}\left(x_a\right) - X_n^{/}\left(x_a + l_a\right)}{\left(\omega_n^2 - \omega^2\right)} \tag{9}$$

To obtain the structural dynamic stiffness, $k_{str}$, calculate the elongation of the PZT wafer:

$$u_{PZT}(t) = u_B(t) - u_A(t) = \frac{h}{2} \sum_n \left[ -X_n^{/}(x_a + l_a) + X_n^{/}(x_a) \right] C_n e^{i\omega t} \tag{10}$$

Introduce modal damping $\zeta_n$ to improve veridicality and use definition (2) to obtain the structural dynamic stiffness as seen by the PZT wafer:

$$k_{str} = \frac{\hat{F}_{PZT}}{\hat{u}_{PZT}} = \left\{ \frac{\left(\frac{h}{2}\right)^2}{\rho A} \sum_n \frac{\left[ X_n^{/}(x_a) - X_n^{/}(x_a + l_a) \right]^2}{\omega_n^2 + 2i\zeta_n \omega \omega_n - \omega^2} \right|^{-1} \tag{11}$$

For pinned-pinned beams, $X_n(x) = A_n \sin(\beta_n x)$, $A_n = \sqrt{2/l}$, $\beta = \left(\omega^2 \rho A / EI\right)^{1/4}$ (Inman, 1996):

$$k_{str}\left(\omega\right) = \left\{ \frac{h^2}{\rho A} \sum_n \frac{\left[ A_n \beta_n(\omega) \sin\left( \beta_n(\omega) \frac{2x_a + l_a}{2} \right) \sin\left( \beta_n(\omega) \frac{l_a}{2} \right) \right]^2}{\omega_n^2 + 2i\zeta_n \omega \omega_n - \omega^2} \right|^{-1} \tag{12}$$

## MODELING OF THE PZT ACTIVE SENSOR

Consider a PZT wafer of length $l_a$, thickness $t_a$, and width $b_a$, undergoing longitudinal expansion, $u_1$, induced by the thickness polarization, $E_3$. The constitutive equations of the PZT material are:

$$\begin{aligned} S_1 &= s_{11}^E T_1 + d_{31} E_3 \\ D_3 &= d_{31} T_1 + \varepsilon_3^T E_3 \end{aligned} . \tag{13}$$

where $S_1$ is the strain, $T_1$ is the stress, $D_3$ is the electrical displacement (charge flux per unit area), $s_{11}^E$ is the mechanical compliance at zero field, $\varepsilon_3^T$ is the dielectric constant at zero stress, $d_{31}$ is the induced strain coefficient, i.e., mechanical strain per unit electric field (Table 1). The mechanical stiffness of the PZT active sensor with respect to an axial force applied in the $u_1$ direction is

$$k_{PZT} = \frac{A_a}{s_{11} l_a}, \tag{14}$$

where $A_a = t_a \cdot b_a$ is the PZT cross-sectional area. Because of the PZT small dimensions, longitudinal wave propagation effects in the PZT wafer are negligible, i.e., the strain induced in the PZT wafer is unaffected by wave propagation effects and hence uniform along the PZT length. The stiffness Equation (14) is used for both static and dynamic regime.

Table 1 Properties of the active-sensor PZT material

| Name | Symbol | Value |
|---|---|---|
| Compliance | $s_{11}$ | $15.2 \cdot 10^{-12}$ Pa$^{-1}$ |
| Dielectric constant | $\varepsilon_3$ | $7.427 \cdot 10^{9}$ F/m |
| Induced strain coefficient | $d_{13}$ | $-125 \cdot 10^{-12}$ m/V |

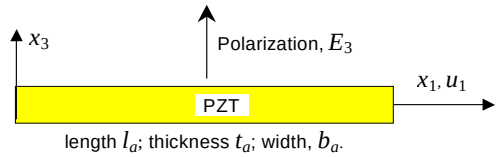


Figure 4 PZT wafer active sensor schematic.

## NUMERICAL EXAMPLE

Consider a uniform beam of $l$ = 100 mm, $h$ = 3 mm, $b$ = 19.6 mm, $E$ = 200 GPa, $\rho$ = 1600 kg/m$^3$, and $\zeta$ = 1%. A PZT wafer active sensor is affixed to the top surface of the beam at $x_a$ = 40 mm. The PZT-wafer active-sensor dimensions are $l_a$ = 4.5 mm, $b_a$ = 4.5 mm, $t_a$ = 0.2 mm.

### Natural Frequencies

The frequency range 100 kHz to 400 kHz was scanned for natural frequencies of the beam (Table 2). This investigation revealed that 9 modes (modes 8 through 17) enclose the frequency range of interest, with the lower mode at 97 kHz setting $N_1$ = 8, and the upper mode at 440 kHz setting $N_2$ = 17. Note that of the 9 modes, only 7 (modes 9 through 16) lie strictly between 100 kHz and 400 kHz (mode 9 is at 123 kHz, and mode 16 at 389 kHz).

Table 2 Frequencies considered for analysis in the 100 kHz to 400 kHz frequency range

| Mode # | 8 | 9 | 10 | 11 | 12 | 13 | 14 | 15 | 16 | 17 |
|---|---|---|---|---|---|---|---|---|---|---|
| Frequency, kHz | 97 | 123 | 152 | 184 | 219 | 257 | 298 | 342 | 389 | 440 |

**Pointwise Structural Stiffness and Dynamic Stiffness Ratio**

Figure 5a shows the pointwise dynamic stiffness, $k_{str}(\omega)$, presented by the beam to PZT exciter. Since the dynamic stiffness is the inverse of the mechanical response, the points of maximum dynamic response (mechanical resonances) correspond to points of minimum dynamic stiffness, and vice-versa. The resonance frequencies corresponding to modes 9 through 16 (123, 152, 184, 219, 257, 298, 342, and 389 kHz) appear as valleys in the dynamic-stiffness magnitude plot (Figure 5a, upper plot). However, these valleys are not always easily identified, as for example the shallow resonance at 219 kHz. (Such shallow resonances are caused by the PZT being placed at a low-curvature point in that particular natural mode of vibration.) A much better resonance identification is obtained through a plot of the real part of the dynamic stiffness. At resonance, the dynamic stiffness is purely imaginary and its real part passes through zero. Hence, smooth crossings of the zero line by the real part of the dynamic stiffness indicate a structural resonance. It is apparent from the lower plot of Figure 5a that the resonance frequencies 123, 152, 184, 257, 298, 342, and 389 kHz are clearly identified as smooth zero-crossing by the real part of the dynamic stiffness.

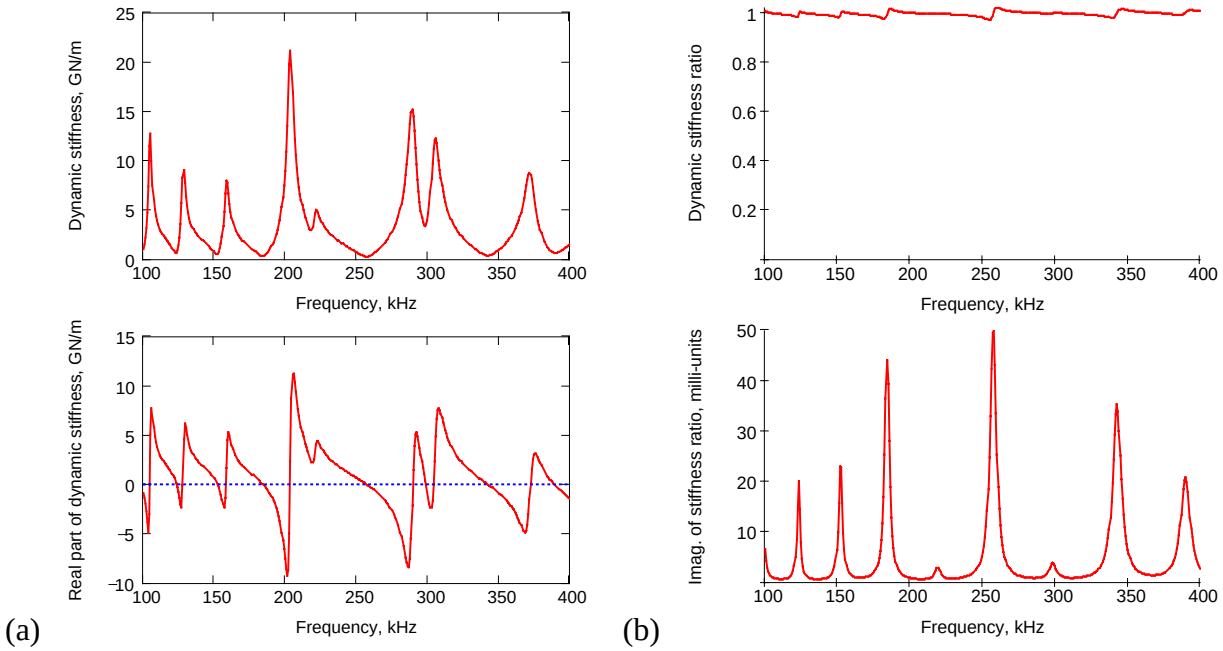


Figure 5 Point-wise dynamic stiffness for $f$ =100 - 400 kHz: (a) structural dynamic stiffness, and real part of structural (continuous line) and PZT dynamic stiffness (dashed line). Dynamic stiffness ratio between structure and PZT wafer showing peaks and zeros in its imaginary part.

Superposed on the lower part of Figure 5a is the dynamic stiffness of the PZT wafer ($k_{PZT}$ = 0.013 GN/m). Outside structural resonances, the value of the PZT stiffness is much lower than the magnitude of the structural stiffness. However, at structural resonances, the real part of the structural stiffness goes through zero and hence becomes comparable with the PZT stiffness. Calculatinge the dynamic stiffness ratio

$$r(\omega) = \frac{k_{str}(\omega)}{k_{PZT} + k_{str}(\omega)} = 1 - \frac{k_{PZT}}{k_{PZT} + k_{str}(\omega)} \ , \qquad (15)$$

one notes that its imaginary part goes through maxima as its denominator goes through minima at structural resonances:

$$\operatorname{Im} r(\omega) = \frac{k_{PZT} \cdot \operatorname{Im} k_{str}}{\left(k_{PZT} + \operatorname{Re} k_{str}\right)^2 + \left(\operatorname{Im} k_{str}\right)^2} \ . \tag{16}$$

This behavior is illustrated in the lower plot of (Figure 5b), which displays clearly defined peaks at the resonance frequencies 123, 152, 184, 219, 257, 298, 342, and 389 kHz. This means that the imaginary part of the dynamic stiffness ratio is a good detector of structural resonances.

Upper part of Figure 5b shows a plot of the dynamic stiffness ratio magnitude. As indicated by the second part of Equation (15), the magnitude of the dynamic stiffness ratio is dominantly equal to unity. Only at resonances does the second term play any role at all, and in this case it is merely a small correction. In the upper plot of Figure 5b, the structural resonances appear as mere glitches, too small to play a reliable detection role. This means that the magnitude of the dynamic stiffness ratio is practically insensitive to the structural resonances and its use, as a resonance detector, would be inappropriate. On the other hand, structural resonances are strongly detected by the imaginary part. This observation is essential to understanding how the electro-mechanical (E/M) impedance of the PZT active sensor couples with the structure and how detection of the structural damage can be achieved. Details of this mechanism are given next.

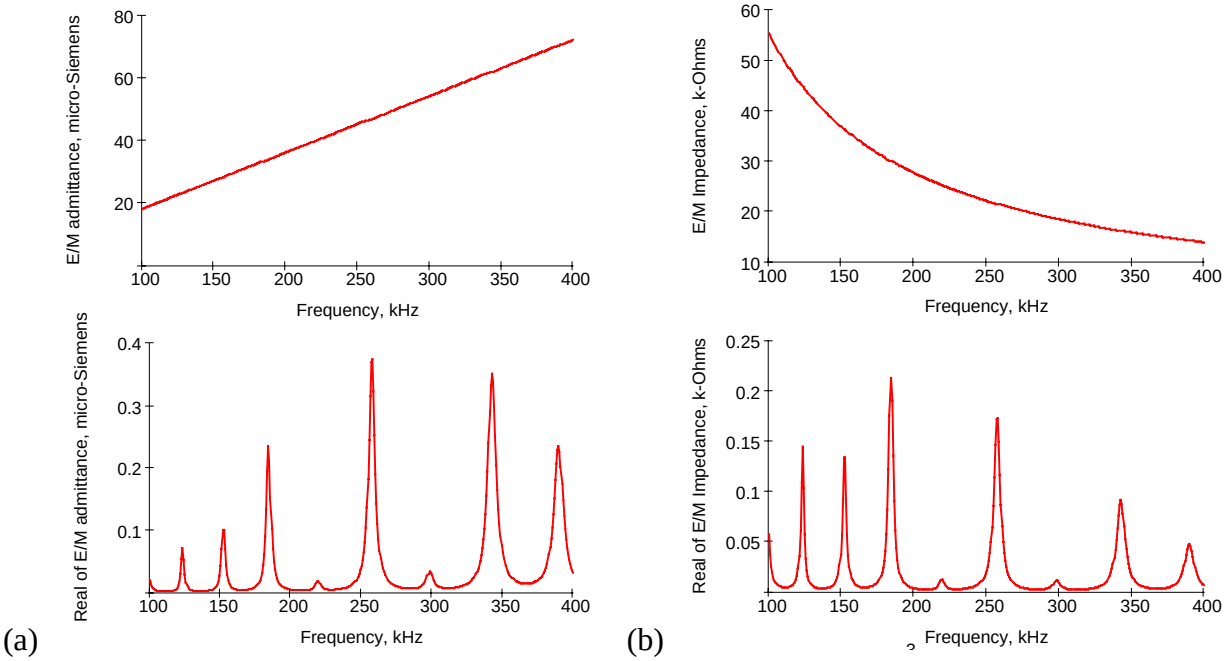


Figure 6 High frequency electrical response of the PZT-wafer affixed to the beam surface: (a) E/M admittance ; (b) E/M impedance. The structural resonances are only reflected in the real part.

**Prediction of E/M Admittance and E/M Impedance Response**

Figure 6 gives the magnitude and real part of the E/M admittance and E/M impedance as would be measured at the electrical terminals of the PZT-wafer active sensor. As predicted by Equation (1), the E/M admittance magnitude (Figure 6a, upper plot) is dominated by the $i\omega C$ component. It varies linearly with frequency and does not display any noticeable changes at the structural

resonance frequencies. The real part of the E/M admittance (Figure 6a, lower plot), though much smaller in value than the E/M admittance magnitude, follows closely the structural-response resonance pattern displayed by the imaginary part of the dynamic stiffness ratio (Figure 5b, lower plot). A similar behavior is displayed by the magnitude and real part of the E/M impedance (Figure 6b). The E/M impedance magnitude is dominated by the capacitive component of the PZT sensor ($1/i\omega C$), and varies as $1/\omega$. The real part of the E/M impedance, on the other hand, follows closely the structural resonance pattern. This indicates that the real parts of the E/M admittance and of the E/M impedance, as measured at the PZT terminals, are good detectors of structural resonances.

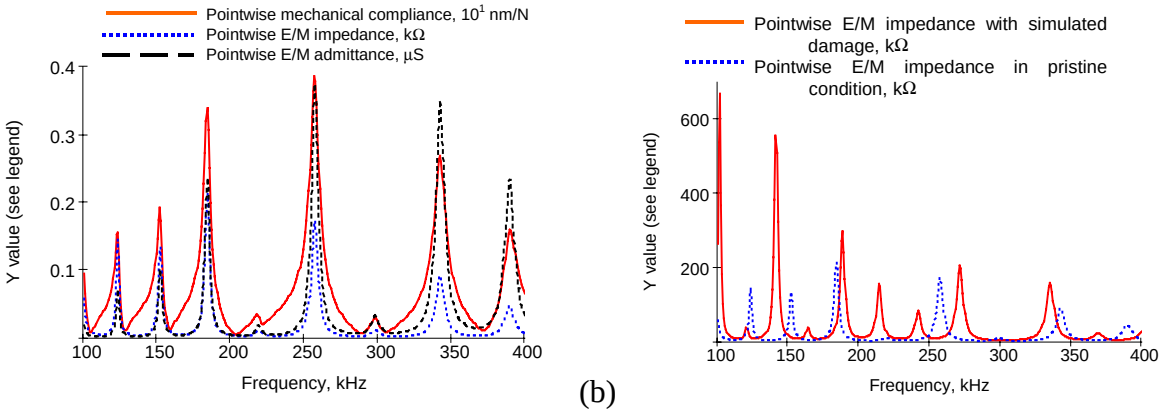


Figure 7 (a) Comparison of pointwise mechanical compliance, E/M impedance, and E/M admittance; (b) Changes in E/M impedance for 45% thickness loss (dilamination/debond/corrosion damage)

### Comparison of Mechanical Response, E/M Impedance, and E/M Admittance Signatures

To summarize these findings, Figure 7a displays superposed the mechanical compliance (structural response), the E/M impedance, and the E/M admittance. It can be seen that both the E/M admittance and the E/M impedance follow closely the structural response and have distinctive peaks at the structural resonances. The E/M impedance sensitivity is stronger at lower frequencies, while the E/M admittance sensitivity is stronger at higher frequencies.

### Effect of Structural Damage

The effect of structural damage (45% thickness reduction) on the E/M impedance signature is presented in Figure 7b. Thickness reduction damage may correspond to corrosion in metallic structures, debond in built-up structures, or delamination in composite structures. The clear difference between the two signatures, pristine and damaged, is apparent. The effect of damage is to shift to the left the resonance frequency peaks, and to increase their amplitude. These E/M impedance signature changes can be used in damage detection.

## CONCLUSIONS

The electro-mechanical (E/M) impedance method has gained acceptance as an effective technique for structural health monitoring, damage detection, and failure prevention. In spite of extensive experimental validation and proof-of-concept demonstrations, little work has been dedicated to its modeling. This paper presented an elementary model for predicting the E/M impedance response of a 1-D beam structure interrogated by a PZT wafer active sensor. The

bending moments induced by the PZT wafer into the beam were considered. Flexural vibration analysis under moment excitation was developed, and the damped normal-modes solution was obtained. A general expressions for pointwise dynamic stiffness to in-plane surface excitation was deduced. Effective stiffness of the PZT wafer was calculated, and the complex stiffness ratio for the PZT-structure interaction was determined. Hence, expressions the complex E/M admittance and E/M impedance were developed.

A numerical example was given to illustrate the method and test its effectiveness. It was found that the real part of the pointwise dynamic stiffness interacts at par with the PZT stiffness at structural resonance frequencies. Pointwise structural resonances were found to be directly reflected in the imaginary part of the complex stiffness ratio, and in the real part of the E/M admittance and E/M impedance. However, the magnitudes of the E/M admittance and E/M impedance were found to be insensitive to structural resonances. Thus, the real parts of the E/M admittance and E/M impedance were singled out as good detectors of structural response. Use of this method for damage detection was also illustrated. When simulated damage was introduced, shifts in the response peaks and modification of peak amplitudes were obtained in the E/M impedance real part response that could be directly traced to damage-induced changes in the structural response.

## ACKNOWLEDGMENTS

The authors gratefully acknowledge the financial support of the contract document # BF 0133 is thankfully acknowledged. Sandia National Laboratories is a multiprogram laboratory operated by Sandia Corporation, a Lockheed Martin Company, for the United States Department of Energy under contract DE-AC04-94AL85000.

## REFERENCES

ANON., *Sonic Bondmaster™*, Staveley NDT Technologies, 421 North Quay St., Kennewick, WA 99336, 1998

CRAWLEY, Edward F.; ANDERSON, Eric H. (1990) "Detailed Models of Piezoceramic Actuation of Beams", *Journal of Intelligent Material Systems and Structures*, Vol.1, No. 1, 1990, pp. 5-25.

CRAWLEY, Edward F.; de LUIS, Javier (1987) "Use of Piezoelectric Actuators as Elements of Intelligent Structures", *AIAA Journal*, Vol. 25, No. 10, pp. 1373-1385, 1987.

ESTEBAN, J.; LALANDE, F.; ROGERS, C. A. (1996) "Parametric Study on the Sensing Region of a Collocated PZT Actuator-Sensor," *Proceedings, 1996 SEM VIII International Congress on Experimental Mechanics*, 10-13 June, 1996.

GIURGIUTIU, V.; CHAUDHRY, Z.; ROGERS C. A. (1994) "The Analysis of Power Delivery Capability of Induced Strain Actuators for Dynamic Applications," *2nd International Conference on Intelligent Materials*, Williamsburg, VA, 5-8 June 1994, pp. 565-576.

GIURGIUTIU, V.; ROGERS, C. A. (1998) "Recent Advancements in the Electro-Mechanical (E/M) Impedance Method for Structural Health Monitoring and NDE, *Proceedings of the SPIE's 5th International Symposium on Smart Structures and Materials*, 1-5 March 1998, Catamaran Resort Hotel, San Diego, CA, pp. 536-547.

GIURGIUTIU, V.; ROGERS, C. A. (1999) "Modeling of the electro-mechanical (E/M) impedance method applied to a composite beam", Report # USC-ME-LAMSS-99-105, May 29, 1999.

INMAN, J. D. (1996) *Engineering Vibration*, Prentice Hall, 1996.

LIANG, C.; SUN, F. P.; ROGERS C. A. (1996) "Electro-mechanical Impedance Modeling of Active Material Systems," *Smart Materials and Structures*, Vol. 5, pp. 171-186.

LIN, M. W.; ROGERS, C. A. (1993) "Modeling of the Actuation Mechanism in a Beam Structure with Induced Strain Actuators", paper # AIAA-93-1715-CP, 1993, pp. 3608-3617.

LIN, M. W.; ROGERS, C. A. (1994) "Bonding Layer Effects on the Actuation Mechanism of an Induced Strain Actuator/Substructure System", *SPIE Vol. 2190*, 1994, pp. 658-670.

ROGERS, C. A.; GIURGIUTIU, V. (1997) "Electro-Mechanical (E/M) Impedance Technique for Structural Health Monitoring and Non-Destructive Evaluation", Invention Disclosure No. 97162, University of South Carolina Office of Technology Transfer, July 1997.

ROGERS, Craig A. (1993) "Structural Impedance Modification and Energy Consideration for Structural Control", *Technical Memorandum of PWRI No. 3217, ISSN 0386-5878*, May 1993, pp. 355-380.

TIMOSHENKO, S. (1955) *Vibration Problems in Engineering*, D. Van Nostrad Company, Inc., 1955.

WANG, Bor-Tsuen; ROGERS, Craig A. (1991) "Modeling of Finite-Length Spatially-Distributed Induced Strain Actuators for Laminate Beams and Plates", paper # AIAA-91-1258-CP, 1991, pp. 1511-1520.

Electro-mechanical (E/M) impedance is a powerful structural identification and health monitoring (SHM) technique that allows for inferring high-frequency structural dynamic characteristics directly by interrogating a network of embedded piezoelectric active sensors. In recent years, there has been a considerable interest in expanding range of applications of the electromechanical impedance technique, its synergistic integration into complementary SHM methodologies, and miniaturizing the associated impedance measurement circuitry.Â  The electro-mechanical model of a piezoelectric impedance sensor is discussed and development of the electrical circuit representation of the sensor-structure interaction is presented. Hence, the complex electro-mechanical impedance and admittance are deduced. A numerical example is given to illustrate the method and test its effectiveness. At structural resonance frequencies, the interaction between the real part of the structural dynamic stiffness and the PZT stiffness is directly reflected in the real part of the electro-mechanical impedance. The same behavior is also found in the electro-mechanical admittance. Both reflect the change in structural response, due to the presence of damage and internal flaws.